北海道大学工学部研究報告
第125号（昭和60年）

Bulletin of the Faculty of Engineering,
Hokkaido University. No. 125 (1985)

# Wave and Geometrical Approach in Hologram Aberration

Yukihiro ISHII

(Received November 30, 1984)

**Abstract**

The diffraction patterns suffering from hologram aberrations are of considerable interest because these factors permit an assessment of hologram imagery. The aberrated diffraction patterns are approached from two different items; that of the wavefront matching with the diffraction integral and ray tracing. This paper is concerned with the combined influence of diffraction and aberrations by using a holographic technique on a reconstructed image from a hologram. The ray-traced spot diagrams are also shown.

## 1. Introduction

In general, optical holography involves the recording of the interference pattern of two laser light beams that are incident on a recording material. In this paper, the equations expressing the hologram aberration in thick medium are derived in which the general theory contains the theory of thin hologram aberration as special cases, viz. those of small thickness or low spatial frequency. The wavefront matching analysis among hologram aberrations involves that of a hologram of which the image wavefront is compared with an ideal spherical or plane wavefront. The relationship between ray aberration and wavefront aberration using a ray tracing is presented. The ray-tracing analysis of holography is closely related to the wavefront matching analysis in that the rays are simply vectors normal to the wavefront following the eikonal equation[1]. This analytical process does not take into account the boundary diffraction effects. Experimental results are shown.

## 2. Wave and geometrical optics in hologram aberration

In this section, theoretical expressions for thick hologram aberrations using the propagated angular spectrum[2] are briefly presented.

Shown in Fig.1 is the geometry used for the analysis of hologram aberration. The arbitrary illumination is assumed to come from point sources subscripted by the dummy q which is replaced by i, c, o and r respectively to denote the position of the image, reconstruction, object and reference beams. The variable $R_q$ is the radial distance along the principal ray from the hologram center O to the point source Q. The projection of the line $R_q$ onto the y-z plane forms an angle $\beta_q$ with respect to the x-z plane and likewise, the

Department of Applied Physics

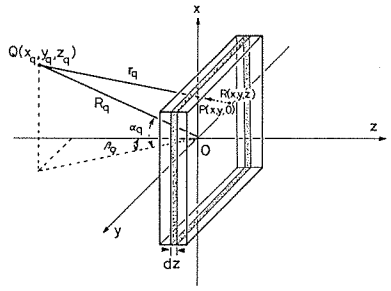


**Fig.1** Coordinate location in thick hologram geometry.

projection of that forms $\alpha_q$ with respect to the y-z plane. An attempt is made to fit the form of summing up all of the elementary contributions of the amplitude propagated from the thin aperture dz with direction cosines $p_q$, $q_q$ of plane waves over the thickness t of the emulsion into the form of $\exp(ik_c r_i)$ as follows,

$$\exp\{ik_c r_i(x,y,0)\}=\frac{1}{t}\int_0^t \exp(ik_c z)\exp(ik_c r_c)_* \mathrm{F}^{-1}[\exp\{-ik_c z(p_c^2+q_c^2)/2\}]\exp(\pm ik_o r_o)_* \mathrm{F}^{-1}[\exp\{\mp ik_o z(p_o^2+q_o^2)/2\}] \exp(\mp ik_o r_r)_* \mathrm{F}^{-1}[\exp\{\pm ik_o z(p_r^2+q_r^2)/2\}]_* \mathrm{F}^{-1}[\exp(ik_c \sqrt{1-p_i^2-q_i^2}\,z)]dz. \tag{1}$$

where $k_q=2\pi/\lambda_q$ is the wave number with the wavelength $\lambda_q$, and $r_q$ is the distance from Q to an arbitrary point P on hologram surface, $_*$ denotes convolution, $\mathrm{F}^{-1}$ is the inverse Fourier transform, and the upper sign indicates a true or the lower sign a conjugate image. Eq. (1) is closely related to the expression for thick hologram imagery. For the propagated distance $z$ approaching zero or for $p_q^2+q_q^2\simeq 0$ (vanishingly low spatial frequency), the wavefront matching analysis of hologram imagery[3] in thin medium is established in the form,

$$\exp(ik_c r_i)=\exp(ik_c r_c)\exp(\pm ik_o r_o)\exp(\mp ik_o r_r), \tag{2}$$

since $\mathrm{F}^{-1}$ [exp(..)] in eq. (1) becomes $\delta(x, y)$ denoting the Dirac delta function. The phase function $\phi_{i,s}$ of the image beam representing the gaussian reference spherical wave is written by

$$\phi_{i,s}=\frac{2\pi}{\lambda_c}\{\sqrt{(x-x_i)^2+(y-y_i)^2+R_i^2-(x_i^2+y_i^2)}-R_i\}. \tag{3}$$

Returning to eq. (2) and referring to Fig.1, matchings of second-order phase terms and of the remainder of the second-order phase terms in eq. (2) using a binomial expansion of $r_q$ about $R_q$ yield a gaussian focus. The wavefront aberration $W(x, y)$ may be given by

$$\frac{2\pi}{\lambda_c}W=\phi_i-\phi_{i,s}, \tag{4}$$

using $\phi_i = k_c r_i$, and $\phi_{i,s}$ contains the phase terms having various orders of the gaussian reference wave. The third-order aberrations which correspond to the Seidel aberrations[1], being an imperfect match as described in eq. (4) between the third-order phase terms of the right side of eq. (2) and the third-order phase terms of the gaussian reference wave of eq. (3), separate into the three usual types:

$$W(x,y) = \Delta_S + \Delta_C + \Delta_A$$
$$= -\frac{1}{8}(x^2+y^2)^2 S + \frac{1}{2}(x^2+y^2)xC - \frac{1}{2}x^2 A, \tag{5}$$

where $S$. $C$ and $A$ are the coefficients of respective aberrations and $\Delta(x, y)$ is the corresponding wavefront aberration. Expansion[4] of the square roots in $r_q$ about $z_q$ leads to distortion and field corvature. Here, for the sake of the experiments, it is assumed that the hologram construction and reconstruction geometry is confined to the $x$, $z$ plane. Considerable simplification is possible and the hologram aberrations correspond to those of a rotationally symmetric optical system. In terms of experimental parameters, the aberration coefficients are given by

$$b\left(\frac{x_q^k}{R_q^3}\right) \equiv \frac{x_c^k}{R_c^3} \pm \mu\left(\frac{x_o^k}{R_o^3} - \frac{x_r^k}{R_r^3}\right) - \frac{x_i^k}{R_i^3}\ , \tag{6}$$

where the wavelength ratio $\mu$ is $\mu = \lambda_c/\lambda_o$, and the superscript k stands for the power and k=0,1 and 2 correspond to spherical aberration (S), coma (C) and astigmatism (A), respectively.

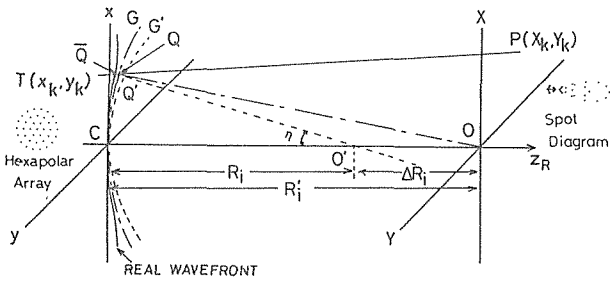


**Fig.2** Schematic illustration of ray input in hologram plane and ray-traced spot in defocused image plane. Also shown are wavefront and ray aberrations.

Ray tracing through a flat hologram aberrated with the wavefront of eq. (4) is as in the following procedure. A ray enters the hologram plane perpendicularly at the point $(x_k, y_k)$ and intersects the defocused image plane at the point $(X_k, Y_k)$ at the distance $R_i + \Delta R_i$ from a hologram center C; subscript k stands for the k-th ray in the input aperture and $\Delta R_i$ denotes a defocus. In Fig.2, let $R_i$ and $R_i'$ $(=R_i+\Delta R_i)$ denote the radii CO′ and CO of a gaussian reference sphere G′ centered on a point O′ and a reference sphere G on the longitudinal defocused point O, respectively. Such a change of the reference sphere will cause a new focus where this is to the right of the old one. The wavefront aberration due to the focal shift denoting the optical path length [QQ′] yields

$$[QQ'] \simeq \frac{\Delta R_i}{2R_i^2}(x^2+y^2). \tag{7}$$

The phase function $\phi$ to be ray-traced is put in the form

$$\phi = \frac{2\pi}{\lambda_c}W + \frac{2\pi}{\lambda_c}\sqrt{x^2+y^2+\{z_R-(R_i+\Delta R_i)\}^2}, \tag{8}$$

which is composed of the aberrated wavefront and a new reference sphere of the second term with a radius equal to $R_i+\Delta R_i$.

Now, we consider the geometrical optics which describes the propagation of the wavefront. On account of eikonal equation, the direction cosines of image ray propagating in air can be computed from the partial derivatives of the phase function of eq. (8). Thus, the relationship between the wavefront aberration $W$ and the transverse ray aberrations $X_k$ and $Y_k$, given by

$$X_k \simeq -(R_i+\Delta R_i)\frac{\partial W}{\partial x} \text{ and } Y_k \simeq -(R_i+\Delta R_i)\frac{\partial W}{\partial y}. \tag{9}$$

We shall present the complex amplitude $v(X, Y)$ at a observation point P of the aberrated diffraction pattern shown in Fig.2. The disturbance at Q is given by $A\exp\{ik_c(W-R_i')\}/R_i'$ where $A/R_i'$ is the amplitude at Q. Then, the diffraction integral based on the Huygens-Fresnel principle is represented by

$$v(X, Y) = \frac{1}{i\lambda_c}\frac{A}{R_i'^2}\exp\left(ik_c\frac{X^2+Y^2}{2R_i'}\right)\iint_G \exp\left[ik_c\left\{W-\frac{\Delta R_i}{2R_i^2}(x^2+y^2)\right\}\right]$$
$$\cdot\exp\left\{-i\frac{k_c}{R_i'}(xX+yY)\right\}dxdy. \tag{10}$$

## 3. Experimental verification

We shall look for the experimental conditions under which the overall holographic process produces the desired wavefront aberrations. The desired amount of wavefront aberration is determined by the aberration at the margin of a square or a circular aperture. Diffraction patterns of a square aperture having a third-order coma have been numerically investigated[5]. Following eq. (6), in setting $S=A=0$, the following equation holds $R_o=R_r$, $\alpha_o=-\alpha_r$, and $R_c=R_i=\infty$, $\alpha_o=\alpha_i=-\alpha_c$ where the gaussian image properties of the hologram for the true image were taken into account. When a square aperture having width $2a$ is used, the wavefront aberration at the position $x=y=a$ is represented by $\Delta_c=(2a^3\sin\alpha_o)/R_o^2$ using eq.(5). Substitution of $\alpha_o=-\alpha_r=10^\circ$ and $R_o=R_r=189$ mm into the above quoted equation produces the values of $\Delta_c=1.92\lambda$ and $0.983\lambda$ for $a=5$ mm and 4 mm, respectively, using the wavelength of He=Ne laser, $\lambda_o=\lambda_c=633$ nm. In order to combine coma and astigmatism, letting $S$ and $\alpha_i$ be equal to zero and using eq.(5), the following equation holds $C=(\sin\alpha_c)/(1/R_c^2-1/R_o^2)$ and $A=(\sin\alpha_c)\{\sin\alpha_c/R_c-(\sin\alpha_o+\sin\alpha_r)/R_o\}$ for both real and virtual images. For a real image, the values $\Delta_c=-0.295\lambda$ and $\Delta_A=0.953\lambda$ are derived from eq.(5) for $\alpha_c=13^\circ4'$ with the circular aperture $2a=10.94$ mm.

We present the experimental results of aberrated diffraction patterns compared with

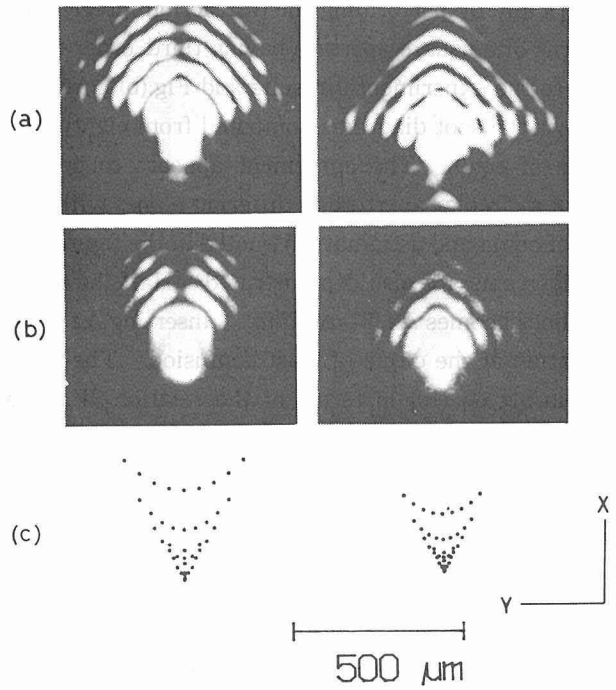


**Fig.3** Results for $\Delta_c=1.92\lambda$ (left) and $0.983\lambda$ (right) of a square aperture. (a)Experimental. (b)Numerical. (c)Ray tracing.

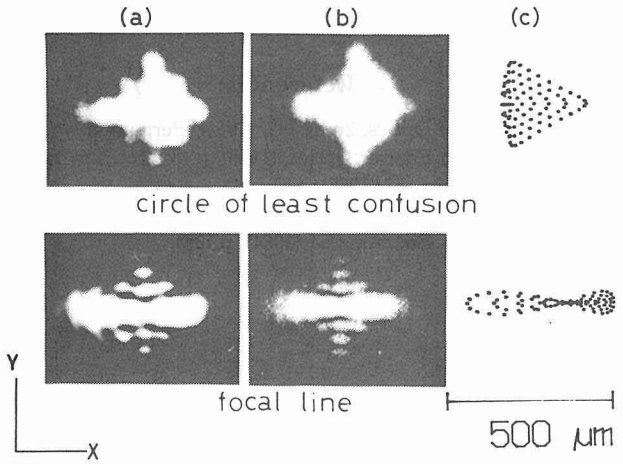


**Fig.4** Results for the combination of coma $\Delta_c=-0.295\lambda$ and astigmatism $\Delta_A=0.953\lambda$ at the circle of least confusion (above) and at a focal line (below). (a)Experimental. (b)Numerical. (c) Ray tracing.

those obtained numerically by performing the diffraction integral of eq. (10). Fig.3 shows the diffraction patterns of a square aperture having third-order coma stated in the figure. Fig.3(a) corresponds to the experimental results and Fig.(b) corresponds to the calculated results. Fig.3(c) shows the spot diagrams computed from eighty-one ray input forming a square grid in terms of eq.(9). The agreement appears to be good. Fig.4 shows the diffraction patterns of a circular aperture at differing planes with a shift of focus suffering from a combination of coma and astigmatism quoted in the figure. Numerical results and corresponding spot diagrams are also demonstrated. Half the astigmatic difference $\Delta z/2$ between two focal lines bcomes $\Delta z/2=\Delta_A R_1^2/a^2$. Inserting $\Delta z/2$ into $\Delta R_1$ in eq. (7) yields the wavefront aberration at the circle of least confusion. The pattern above in Fig.4 (b) is obtained by calculating eq. (10) in terms of the relation $W=\Delta_A x^2/a^2+\Delta_c x(x^2+y^2)/a^3$ setting $\Delta R_1=\Delta_A R_1^2/a^2$. The pattern below in Fig.4 (b) is obtained by calculating eq. (10) in terms of the above stated relation setting $\Delta R_1=0$.

## 4. Conclusion

This paper presents the diffraction patterns of a square or a circular aperture suffering from third-order hologram aberrations. The patterns observed are compared with the theoretical ones which are obtained numerically by the theory of thin hologram aberration. These results illustrate both effects of diffraction and aberrations on a point image. On the other side, the approach to geometrical optics is described as the spot diagrams, showing the influence of aberration only, calculated by the ray-tracing program.

The author wishes to thank Prof. K. Murata for helpful encouragement during the course of this work.

### References:

1) Born, M., Wolf, E.: Principles of Optics, 2nd. ed., (1964), Pergamon.
2) Goodman, J. W.: Introduction to Fourier Optics, (1968), p.48, McGraw-Hill.
3) Champagne, E. B.: J. Opt. Soc. Am., 57 (1967), p.51.
4) Meier, R. W.: J. Opt. Soc. Am., 55 (1965), p.987.
5) Barakat, R., Houston, A.: J. Opt. Soc. Am., 54 (1964), p.1084.